J. Membrane Biol. 136, 191–197 (1993)

The Journal of
Membrane
Biology

Structural Features of a Multisubstate Cardiac Mitoplast Anion Channel: Inferences from Single Channel Recording

K.A. Hayman, R.H. Ashley
Department of Biochemistry, University of Edinburgh, George Square, Edinburgh EH8 9XD, Scotland, UK

Received: 12 March 1993/Revised: 12 July 1993

Abstract. Ion channels from sheep cardiac mitoplast (inverted inner mitochondrial membrane vesicle) preparations were incorporated into voltage-clamped planar lipid bilayers. A low-conductance anion channel (~40 or ~85 pS in symmetric 300 or 550 mM choline Cl, respectively), characterized by the presence of two well-defined substates, at ~25 and ~50% of the fully open level, was studied in detail. The substate behavior was consistent with a multibarrelled channel containing four functionally coupled pores. At negative (*cis-trans*) membrane potentials, the putative protomers appeared to gate with substantial positive cooperativity, accounting for the apparent absence of a ~75% sublevel. At positive holding potentials, allosteric protomer interactions were more complicated, and the channel complex could be modeled as a dimer of dimers. The protochannels in one dimer ("dimer A") appeared to open independently of each other, and with a relatively high probability, while the monomers comprising the second dimer ("dimer B") were functionally coupled, could only open if both protomers in dimer A were open, and closed as soon as one of the monomers in dimer A shut. The channels also displayed Ca^{2+}- (and Mg^{2+}-) sensitive rectification related to bilayer lipid surface charge. By assuming that Ca^{2+} acted solely by screening surface charge, the membrane surface potential profile was used as a "microscopic ruler" to place one mouth of the channel within 10–11 Å of the bilayer surface.

Key words: Anion channel — Membrane potential — Mitochondrion — Rectification — Substate — Surface charge

Correspondence to: R.H. Ashley

Introduction

The preceding paper (Hayman, Spurway & Ashley, 1993) described the incorporation into planar lipid bilayers of anion channels from sheep cardiac mitoplast (inner mitochondrial membrane vesicle) preparations. The channels were particularly rich in subconductance states between the predominant (in this case, the 100%) open state, and the shut state. Substates (reviewed recently by Fox, 1987) may in principle arise from many different mechanisms, including changes in the conformation of an open pore, or the availability of alternative permeation pathways in the same protein (a "multibarrelled" pore). In some channels, for example the sarcoplasmic reticulum Ca^{2+}-release channel (Wagenknecht et al., 1989), and bacterial porins (Jap & Walian, 1989), a multibarrelled pore has been identified on firm structural grounds (EM single-image reconstruction, X-ray and electron crystallography). However, information concerning the three-dimensional structure of most channel proteins is very limited, and likely to remain so in the near future because of the technical problems associated with their crystallization.

In the absence of much structural information, heavy reliance has traditionally been placed on the interpretation of single channel records in terms of predictive structural models. In this report, the "low-conductance" anion channels identified in the previous paper (Hayman et al., 1993) were studied in detail. Interestingly, they were found to insert asymmetrically into the bilayer such that one face was located only about 1 nm from the membrane surface (as inferred from the effect of membrane surface potential on ion permeation), and while they also exhibited gating behavior consistent with a

multibarrelled channel containing four functionally coupled pores, the allosteric subunit interactions involved appear to have been quite complicated.

Materials and Methods

The preparation of sheep heart mitochondria (Toth, Ferguson-Miller & Suelter, 1986) and inner membrane (mitoplast membrane) vesicles (Chan, Greenwalt & Pedersen, 1970; Williams & Pedersen, 1986), together with the techniques used for planar bilayer reconstitution, and all the materials used, were the same as those described in detail in the preceding paper (Hayman et al., 1993). The *cis* bilayer chamber continued to be voltage-clamped with respect to the *trans* chamber, which was grounded, and all potentials are reported as *cis-trans*. Recordings were carried out in symmetric choline Cl or symmetric KCl, except where stated, and solutions were buffered with 5 mM Tris/HEPES mixtures to a pH of either 8.8 or 7.4. EGTA-buffered free Ca^{2+} (and Mg^{2+}) concentrations were calculated by incorporating the appropriate equilibrium constants for all the relevant reactions (after correcting pH to proton concentration) into an iterative computation based on the procedure described by Perrin and Sayce (1976). Single channel currents were minimally low-pass filtered (cut-off frequency 10 kHz), and stored on a digital tape recorder. The data were post-filtered at 40–200 Hz (-3dB point of an 8-pole Bessel filter for data reconverted to analogue format, or a digital Gaussian filter), and analyzed as described in Results, using pCLAMP and Axotape software (Axon Instruments), supplemented by our own programs. For steady-state, appropriately filtered data, channel amplitudes could easily be measured to an accuracy of 0.05 pA where required.

Results

Bilayer Incorporation of Low-Conductance Anion Channels

Low-conductance anion channel activity was obtained in both palmitoyl-oleoly phosphatidylethanolamine/palmitoyl-oleoyl phosphatidylserine (POPE/POPS, each 50%, w/w) bilayers, or all-POPE bilayers, and always exhibited the characteristic substates, at ~25 and ~50% of the fully open state, described earlier for *s*mall *m*itoplast *a*nion *c*hannels (SMAC, Hayman et al., 1993). The fully open (100% state) conductance, in the presence of 2 mM symmetric Ca^{2+}, was 85 ± 9.2 pS (mean ± SD, n = 6) in symmetric 550 mM choline Cl, 38 ± 6.6 pS (mean ± SD, n = 4) in symmetric 300 mM choline Cl, and 97 ± 14 pS (mean ± SD, n = 7) in symmetric 300 mM KCl. In experiments in which selected channels were exposed to asymmetric solutions (e.g., 550 *vs.* 50 mM choline Cl), reversal potential measurements (analyzed by using the equations of Hodgkin & Katz, 1949) confirmed that the channels were poorly selective between anions and cations (e.g., $P_{Cl^-}/P_{choline^+} \sim 11$), as previously described (Hayman et al., 1993).

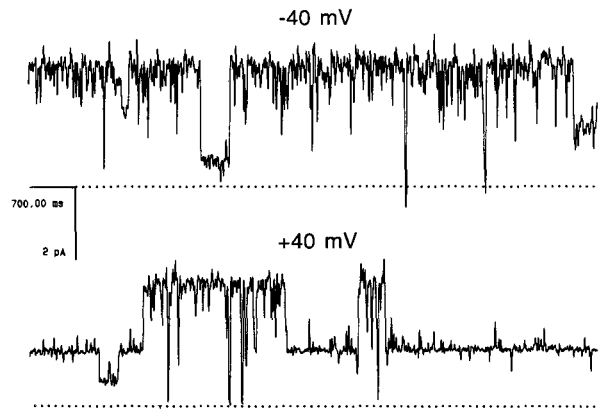

Fig. 1. Voltage-dependent substate behavior. Representative single channel recordings in symmetric 550 mM choline Cl (with 2 mM added Ca^{2+}), to illustrate reduced appearance of the fully open state at positive potentials. The infrequent closures are typical.

Voltage-dependent Substate Behavior

Channel open probabilities, including entry into the ~25 and ~50% substates, were markedly voltage dependent. Occupancy of the fully open (100%) state was substantially reduced at positive holding potentials (Fig. 1). This behavior was largely unaffected by Ca^{2+}, or by changes in pH between 8.8 and 5.5 (*results not shown*). The same effect was seen in each of over 100 experiments, and on switching potentials it clearly occurred rapidly, appearing as soon as the bilayer capacitative transient had ceased to saturate the opamp of the *I/V* converter (i.e., within 10–100 msec). Figures 2 and 3 show longer examples of another channel recording at ±50 mV, with accompanying amplitude histograms. While the marked effect of membrane potential was obvious even in relatively short channel recordings, detailed analysis was only carried out on long segments of uninterrupted data (normally 2–3 min). Open state probabilities, obtained by integrating amplitude histograms, changed abruptly around zero mV as the holding potential was varied. Detailed results from four experiments are shown in Fig. 4, where the 25 and 50% substate open probabilities have been combined for clarity. This switch in gating behavior was mainly attributable to a decrease in the number of apparent transitions between the 50% substate and the fully open state at positive membrane potentials, while transitions between the 25 and 50% substates increased, as shown in Fig. 5. The frequency

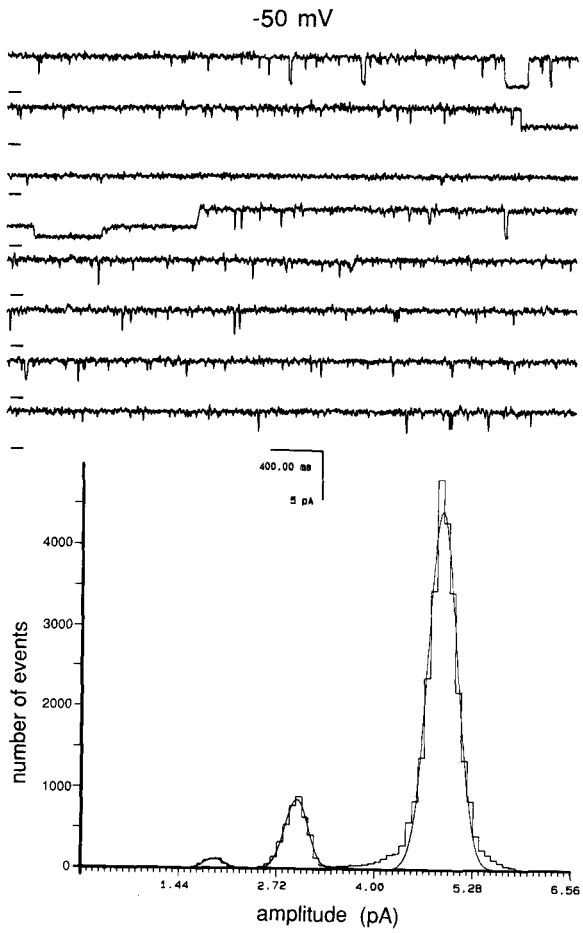

Fig. 2. Single channel recording and amplitude histogram (−50 mV). A 33 sec recording at −50 mV in symmetric 550 mM choline Cl/2 mM $CaCl_2$, filtered at 100 Hz (upper traces, closed level marked —), was sampled at 1 kHz to construct an all-points amplitude histogram (lower graph). This is fitted to three Gaussian curves. Note very low closed probability in this recording (closed level amplitude set to 1.00 pA).

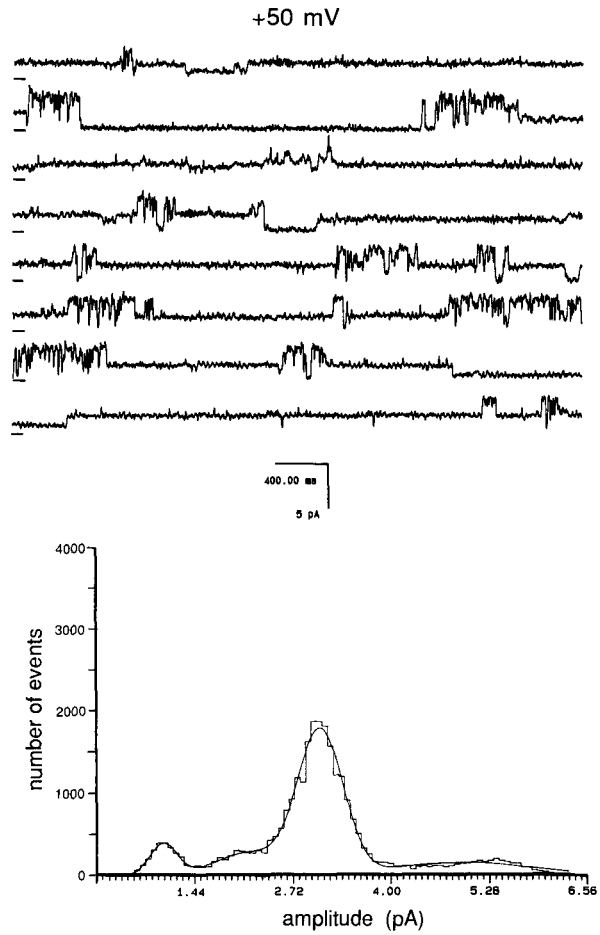

Fig. 3. Single channel recording and amplitude histogram (+50 mV). Same channel as Fig. 2, now recorded at +50 mV; other details unchanged except that the amplitude histogram shows all four Gaussian peaks (closed level amplitude again set to 1.00 pA). Note the increased prominence of substates at the expense of the fully open state.

limitations of the bilayer system prevented the detection of states lasting < 5 msec.

Evidence for a Multibarrelled Pore

The presence of substates at 25 and 50% of the main conductance level was strongly suggestive of a "multibarrelled pore" mechanism. The apparent absence of a 75% level could be accounted for if single channels comprised four protochannels which opened cooperatively, so that the 75% substate only occurred rarely. It will also have been attenuated by the frequency limitations of the bilayer recording system. Careful inspection of the data at negative holding potentials did suggest very infrequent residence (for less than ~1% of the total recording time)

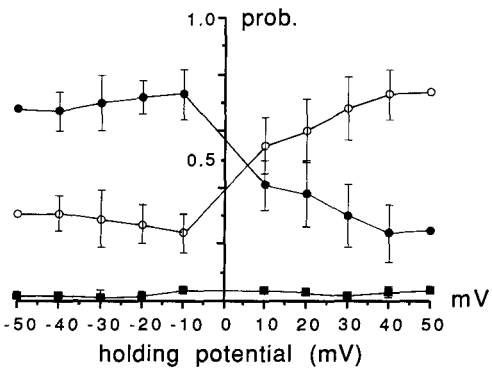

Fig. 4. Comparison of substate frequencies. Data from recordings in symmetric 550 mM choline Cl. Shown ± SEM (n = 4 independent experiments), to compare probabilities (*prob*) of observing main state (●), closed state (■) and substates (○), between ± 50 mV. The substate probabilities have been combined for clarity, and the lines have no significance.

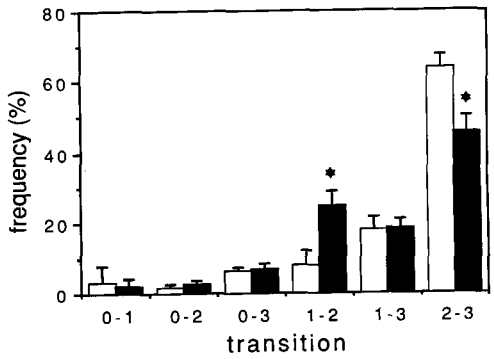

Fig. 5. Comparison of transition frequencies. Transitions between closed (0), fully open (3), 25% (1) and 50% (2) levels in symmetric 550 mM choline Cl are compared for −40 mV (open bars) and +40 mV (filled bars). Data from four independent experiments, shown ± SD. Asterisks indicate significant differences ($P < 0.01$, unpaired t-tests).

in an apparent 75% substate lasting up to a few msec on each occasion (*not shown*). The binomial distribution has been modified to incorporate simple pairwise cooperation between events (the additive generalization of the binomial distribution, Altham, 1978, applied to multichannel records by Glasebey & Martin, 1988):

$$P_i = n!/[i!(n - i)!] \cdot p^i(1 - p)^{n-i} \cdot [1 + [c/2p(1 - p)]\{(i - np)^2 + i(2p - 1) - np^2\}]$$

where the probability of observing the ith level (P_i) for $n = 0, 1, \ldots 4$ protochannels is found by correcting protochannel open probability (p) by the cooperativity factor c. Data were fitted to this distribution by maximizing the likelihood of $\Sigma(F_i) \ln(P_i)$, where F_i was the relative residence in sublevel i. The predicted distributions matched the data well at negative holding potentials, as illustrated in Fig. 6. Mean "cooperativity," averaged over 15 potentials for four channels, was +0.41 ± 0.05 (mean ± SD, n = 15), with a mean protochannel open probability of 0.85 ± 0.06 (mean ± SD, n = 15). However, this model clearly could not apply to the data obtained at positive holding potentials, where the appearance of the maximum conductance level is *reduced* (e.g., Fig. 1, lower trace, and Fig. 3).

The marked change in gating behavior around zero mV could still be accounted for by a four-subunit model at positive potentials, if each tetramer comprised two functionally dissimilar dimers (a dimer of dimers, DoD) which continued to show intersubunit allosteric interactions. In "dimer A," the opening of individual protochannels is held not to be constrained in any way (although more complicated models could, for example, still include positive cooperativity), while in "dimer B" both protomers must open and close together, i.e., they are *very* tightly functionally coupled. In addition, they can only open if *both* promoters in dimer A are already open. Accordingly, data were fitted to the following distribution, where q_j is the probability of the jth open conformation (i.e., j = 1, 2, or 3 for monomer 1 of dimer A, monomer 2 of dimer A, or dimer B):

Probability of no protochannel open $= [(1 - q_1)(1 - q_2)]$ probability of one protomer open $= [(q_1(1 - q_2) + q_2(1 - q_1)]$	DoD cannot evolve
probability of two protomers (dimer A) open $= [q_1q_2(1 - q_3)]$	DoD possible but absent
probability of dimer of dimers open $= [q_1q_2q_3]$	DoD present

Although approximate analytical solutions are obviously possible when q_1 is set to q_2, best fits were in fact obtained by maximum likelihood analysis, using a modification (Box, 1965) of the Simplex direct search algorithm. In each of three channels examined in detail (at a total of 12 positive holding potentials), the calculated best-fit open probabilities fell into a pattern of two relatively high p, similar to those derived in the cooperative model at negative potentials (Fig. 6), accompanied by a lower p representing the final dimerization step to the DoD state. Representative data from a single channel are shown in the Table. Consistent with this overall interpretation, careful inspection of single channel recordings obtained at positive holding potentials showed no evidence for a 75% substate.

Asymmetrical Location in Bilayers

Single channel currents through the low-conductance anion channel rectified strongly in the absence of added Ca^{2+}, especially at negative holding potentials, and this was largely reversed by 2 mM Ca^{2+} *cis* but not by Ca^{2+} *trans* (Fig. 7). In a few experiments, rectification was more marked at positive potentials, and could only be relieved by Ca^{2+} *trans* ("reversed" channels). It was possible that the apparent reductions in single channel currents resulted from short-lived, incompletely resolved openings at negative potentials, but only if this applied equally for each substate (Fig. 8). We therefore sought a more realistic explanation for this Ca^{2+}-dependent rectification, based on divalent cation screening of fixed negative charges on the channel protein or membrane lipid.

Maximum reversal of single channel rectification by *cis* Ca^{2+} was generally achieved by 2–10 mM at a pH of 8.8 (Fig. 9, open symbols). In this case,

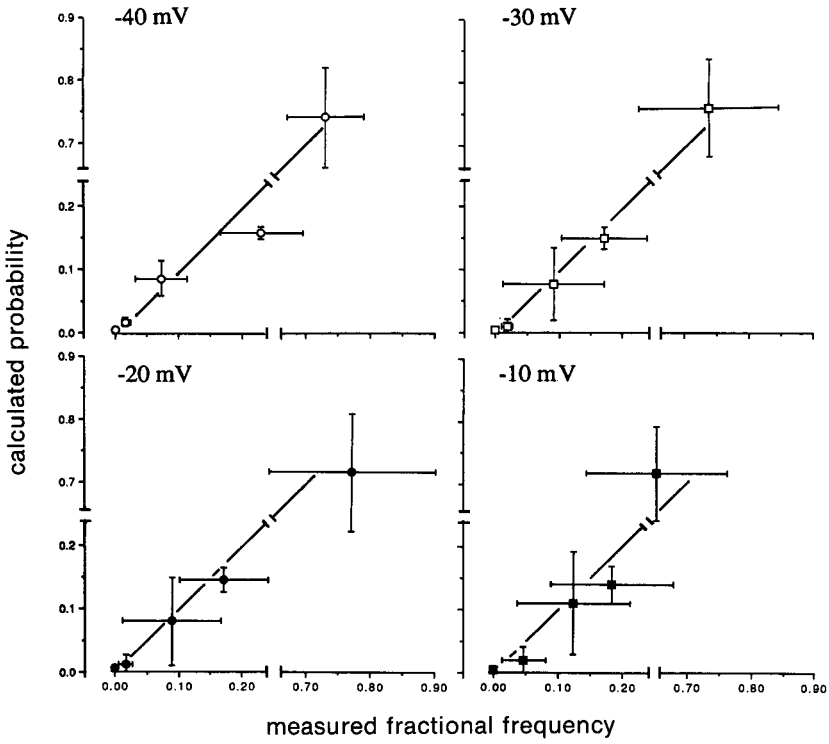

Fig. 6. A correlated binomial model at negative potentials. Data from four independent experiments in symmetric 550 mM choline Cl at four holding potentials (indicated). The measured closed and open state frequencies have been compared to predicted frequencies (calculated probabilities). From the origin in each panel, the conductance states are: 75, 0 (closed), 25, 50 and 100% (fully open or main state conductance). Bars are shown to indicate ± SEM (n = 4), and the lines representing ideal correlation are shown. Note breaks in axes, and low calculated frequencies for the 75% substate at each potential.

Table. A sequential dimer model at positive potentials

Clamp (mV)	State	P_{meas}	P_{fit}	$p_{q(1-37)}$
	Closed	0.07	0.01	
	25%	0.10	0.21	
+40	50%	0.71	0.65	0.88, 0.88, 0.15
	75%	ND	NP	
	100%	0.12	0.12	
	Closed	0.01	0.002	
	25%	0.07	0.08	
+30	50%	0.69	0.68	0.96, 0.96, 0.26
	75%	ND	NP	
	100%	0.24	0.24	
	Closed	0.05	0.03	
	25%	0.25	0.29	
+20	50%	0.54	0.52	0.82, 0.82, 0.22
	75%	ND	NP	
	100%	0.16	0.15	

The measured probabilities (P_{meas}) of closed, 25% (single protomer), 50% (dimer) and 100% (dimer of dimers) conductance states are compared to the predicted distributions (P_{fit}) after determining p_q (for q = protomer, dimer or dimer of dimers states) by maximum likelihood analysis. The model did not predict a 75% substate (NP = not predicted). ND = not detected.

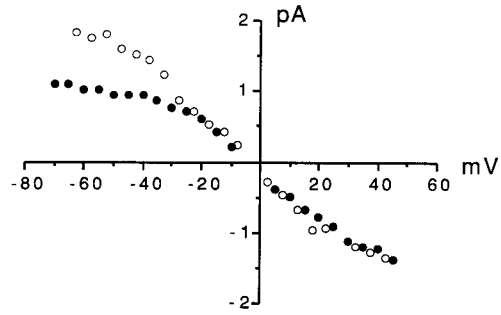

Fig. 7. Single channel rectification, and reversal by Ca^{2+}. I/V relations for the low-conductance anion channel in symmetric 300 mM choline Cl with no added Ca^{2+} (●) and with 1 mM Ca^{2+} *cis*(○). *Trans* Ca^{2+} had no effect.

half-maximal relief in a 1 : 1 (w/w) POPE : POPS bilayer was provided by 320 μM $Ca^{2+} \cdot Mg^{2+}$ also reversed the rectification at similar concentrations, and little rectification was seen in all-POPE bilayers, suggesting that not only was this an effect involving negative surface charge, but also that the charge was associated with the membrane lipid. The reductions in single channel current could be accounted for by the statistical reduction in $[Cl^-]$ (and therefore single channel currents) at the channel entrance on the *cis* side, described by:

$$[Cl^-]_x = [Cl^-]_b \cdot \exp(zF\Psi_x/RT)$$

in which the anion concentration at an entrance located x units from the bilayer, where the surface potential (Ψ_o) has fallen to Ψ_x, is related to the bulk (b) concentration by the Boltzmann distribution. Ψ_x

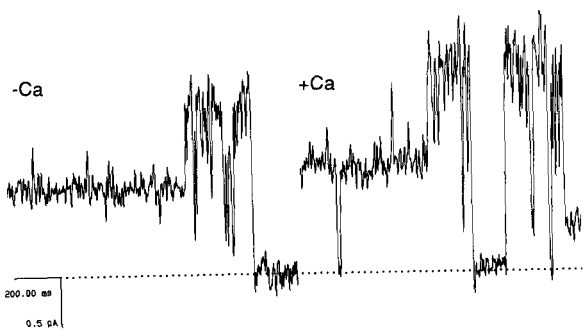

Fig. 8. Effect of *cis* Ca^{2+} at the single channel level. Single channel recording at −30 mV in 550 *vs.* 50 mM choline Cl with no added Ca^{2+} (left) and with 2 mM Ca^{2+} (right), to show proportionate effect of Ca^{2+} on substate amplitudes. Filtered at 60 Hz.

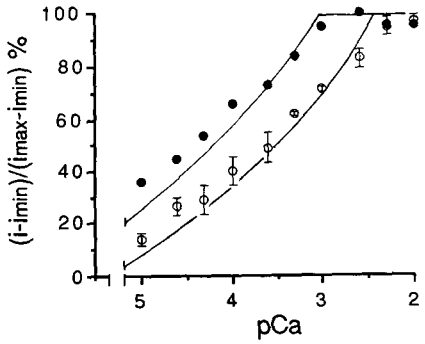

Fig. 9. Reversal of rectification by screening membrane surface charge. Approach of single channel currents (measured at −30 mV in 550 *vs.* 50 mM choline Cl) to maximum amplitude (i_{max}) with increasing *cis* Ca^{2+} in 1 : 1 POPE : POPS membranes at a pH of 7.4 (●) and 8.8 (○) Bars represent ± SEM, $n = 4$ independent experiments. Curves are fitted as described in the text, and for minimum current amplitudes (i_{min}), $[Ca^{2+}]$ was <3 nM.

is also given by appropriate integration of the Poisson-Boltzmann equation (e.g., McLaughlin, 1977):

$$\Psi_x = 2RT/zF \cdot \ln\{[1 + \alpha \cdot \exp(-\kappa x)]/[1 - \alpha \cdot \exp(-\kappa x)]\},$$

where

$$\alpha = [\exp(zF\Psi_o/2RT) - 1]/[\exp(zF\Psi_o/2RT) + 1]$$

and κ is in reciprocal Debyes. The Debye length is the average distance of the counterions from the membrane, and under the experimental conditions used here, was largely determined by the concentration of monovalent ions alone (McLaughlin et al., 1970, Worley et al., 1992). It was calculated to be 0.41 nm. Single channel currents increased by 20% between $Ca^{2+} \sim 0$ and $Ca^{2+} = 10$ mM, and were assumed to be proportional to $[Cl^-]$. The full set of equations were therefore solved iteratively, varying Ψ_o and x. The curves fitted to the data in Fig. 8 were obtained with x set to 1.05 nm (~2.6 Debyes) and Ψ_o set to −82 and −60 mV at a pH of 8.8 and 7.4, respectively, in each case modified by Ca^{2+} screening at a rate of 30 mV per pCa unit (as predicted by the Gouy equation, e.g., McLaughlin 1977, and ignoring any changes in Ca^{2+} binding).

Discussion

Charges in or near the mouths of ion channels are known to exert a large influence on ion permeation, and the *cis* mouth of this anion channel is clearly located close enough to the bilayer to sense the membrane surface potential. Assuming that the effect of Ca^{2+} (and Mg^{2+}) was only mediated by screening membrane surface charge, and the cations had no other effect on the channel protein, such screening allows the surface membrane potential profile to be used as a "microscopic ruler" to show that the *cis* entrance of the channel is located only 10–11 Å from the negatively charged lipid head groups, which are presumably in the plane of the bilayer (while the *trans* entrance is much better insulated). Although not considered explicitly, changes in the *binding* of Ca^{2+} to the fixed charges will have made little difference over most of the range of $[Ca^{2+}]$ used (McLaughlin, 1977). However, currents are not of course strictly proportional to $[Cl^-]$ (in fact, preliminary experiments show that the channel conductance probably saturates at between 150–200 pS in choline Cl). This may well account for the systematic deviation from the fitted lines in Fig. 9, but the intention has not been to provide an exact measurement, and other uncompensated errors are likely to have been more significant. In passing, it should be noted that even at "physiological" pH values POPE carries a small net negative charge, accounting for the slight rectification still seen in "neutral" bilayers.

In preliminary experiments, bilayer surface potentials in the absence of Ca^{2+} were estimated after McLaughlin et al. (1970) by determining the ratio of nonactin-induced K^+-conductances in experimental solutions containing symmetric 10–50 mM KCl before (G*) and after (G_o) screening fixed surface charges with LiCl or $CaCl_2$:

$$\Psi_o = -RT/F \cdot \ln(G^*/G_o)$$

These potentials were found to lie between −50 and −90 mV over the range of conditions used, and

allow calculation of the bilayer surface charge density (σ) from the Gouy equation (McLaughlin, 1977):

$$A\sigma/C^{0.5} = \sinh(-zF\Psi_o/2RT)$$

where $A = 136$ ($[M]^{0.5} \cdot Å^2$) summarizes a number of physical constants at 20°C, and C is the salt concentration. It can be seen that at a pH of 8.8, σ may reach $e^-/0.7$ nm^2 (probably nearer $e^-/0.9$ nm^2 for realistic choline Cl activities). This is close to the maximum theoretical charge density in the bilayers (assuming a lipid cross-sectional area of ~0.7 nm^2) and suggests little if any decane is intercalating between the long axes of the lipid molecules. At this point it should be made clear that divalent cation screening is not implied to be physiologically relevant here (although modifying much lower synaptic surface potentials *asymetrically* may be an important regulator of voltage-dependent *gating*, e.g., Ashley, 1986).

Similarly, while the small anion channel's multisubunit type of substate behavior (also seen for a "double-barrelled" Cl^- channel, Miller & White, 1984, and a "triple-barrelled" K^+ channel, Matsuda, Matsuura & Noma, 1989) may not be particularly related to its role in vivo, it does also lead to a fairly strong prediction of major structural features of the channel protein (although conformational changes in a single pore could in theory give rise to similar electrophysiology, Dani & Fox, 1991). Further tests arising from this model can be developed. For example, the substate behavior, with markedly reduced open probabilities for a "dimer of dimers" state in a sequential gating model at positive (*cis-trans*) potentials, may be sensitive to specific modifiers of charged residues (*cf.* activation and gating in the ryanodine receptor, Orr et al., 1993). Also, examination of channel transitions at much higher resolution (e.g., by patch clamping) would allow another more critical test of the proposed mechanism—is the 75% substate then readily detectable at negative potentials, but still absent at positive potentials?

Although we have not been able to present any evidence for a physiological role for this anion channel, and cannot yet offer any compelling evidence even for its location to the inner mitochondrial membrane, at least two highly specific structural features have been identified by single channel recording alone: one entrance appears to lie unusually close—only about 1 nm—from the surface of the bilayer, and the channel behaves as a four-barrelled pore, or a single-barrelled pore with four gates in parallel.

We are grateful to Richard Martin for his comments on the manuscript, and thank the British Heart Foundation for support.

References

Altham, P.M.E. 1978. Two generalizations of the binomial distribution. *Appl. Stat.* **27**:162–167

Ashley, R.H. 1986. External calcium, intrasynaptosomal free calcium and neurotransmitter release. *Biochim. Biophys. Acta* **854**:207–212

Box, M.J. 1965. A new method of constrained optimization and a comparison with other methods. *Comp. J.* **8**:42–52

Chan, T.L., Greenwalt, J.W., Pedersen, P.L. 1970. Biochemical and ultrastructural properties of a mitochondrial inner membrane fraction deficient in outer membrane and matrix activities. *J. Cell. Biol.* **45**:291–305

Dani, J.A., Fox, J.A. 1991. Examination of subconductance levels from a single ion channel. *J. Theor. Biol.* **153**:401–423

Fox, J.A. 1987. Ion channel subconductance states. *J. Membrane Biol.* **97**:1–8

Glasebey, C.A., Martin, R.J. 1988. The distribution of numbers of open channels in multi-channel patches. *J. Neurosci. Methods* **24**:283–287

Hayman, K.A., Spurway, T.S., Ashley, R.H. 1993. Single anion channels reconstituted from cardiac mitoplasts. *J. Membrane Biol.* **136**:181–190

Hodgkin, A.L., Katz, B. 1949. The effect of sodium ions on the electrical activity of the giant axon of the squid. *J. Physiol.* **108**:37–77

Jap, B.K., Walian, P.J. 1990. Biophysics of the structure and function of porins. *Quant. Rev. Biophys.* **23**:367–403

McLaughlin, S. 1977. Electrostatic potentials at membrane-solution interfaces. *In*: Current Topics in Membranes and Membrane Transport. F. Brunner, A. Kleinzeller, editors. Vol. 9, pp. 71–144. Academic, New York

McLaughlin, S.G.A., Szabo, G., Eisenman, G., Ciani, S.M. 1970. Surface charge and the conductance of phospholipid membranes. *Proc. Nat. Acad. Sci. USA* **67**:1268–1275

Matsuda, H., Matsuura, H., Noma, A. 1989. Triple-barrelled structure of inwardly-rectifying K^+ channels revealed by Cs^+ and Rb^+ block in guinea-pig heart cells. *J. Physiol.* **413**:139–157

Miller, C., White, M.M. 1984. Dimeric structure of single chloride channels from *Torpedo* electroplax. *Proc. Natl. Acad. Sci. USA* **81**:2772–2775

Orr, I., Martin, C., Ashley, R., Shoshan-Barmatz, V. 1993. The interaction of fluorescein isothiocyanate with the ryanodine receptor/Ca^{2+} release channel of sarcoplasmic reticulum. *J. Biol. Chem.* **268**:1376–1382

Perrin, D.D., Sayce, I.G. 1967. Computer calculation of equilibrium concentrations in mixtures of metal ions and complexing species. *Talanta* **14**:833–842

Toth, P.P., Ferguson-Miller, S.M., Suelter, C.H. 1986. Isolation of highly coupled heart mitochondria in high yield using a bacterial collagenase. *Methods Enzymol.* **125**:16–27

Wagenknecht, T., Grassucci, R., Frank, J., Saito, A., Inui, M., Fleischer, S. 1989. Three-dimensional architecture of the calcium channel/foot structure of sarcoplasmic reticulum. *Nature* **338**:167–170

Williams, N., Pedersen, P.L. 1986. Rapid purification of F1-ATPase from rat liver mitochondria using a modified chloroform extraction procedure coupled to HPLC. *Methods Enzymol.* **126**:477–489

Worley, J.F., French, R.J., Pailthorpe, B.A., Krueger, B.K. 1992. Lipid surface charge does not influence conductance or calcium block of single sodium channels in planar bilayers. *Biophys. J.* **61**:1353–1363